

Lawrence Berkeley National Laboratory

LBL Publications

Title

Enhanced nutrient uptake is sufficient to drive emergent cross-feeding between bacteria in a synthetic community.

Permalink

<https://escholarship.org/uc/item/8xk8z4hb>

Journal

The ISME journal, 14(11)

ISSN

1751-7362

Authors

Fritts, Ryan K
Bird, Jordan T
Behringer, Megan G
[et al.](#)

Publication Date

2020-11-01



DOI

10.1038/s41396-020-00737-5

Peer reviewed



Enhanced nutrient uptake is sufficient to drive emergent cross-feeding between bacteria in a synthetic community

Ryan K. Fritts¹ · Jordan T. Bird² · Megan G. Behringer³ · Anna Lipzen⁴ · Joel Martin⁴  · Michael Lynch³ · James B. McKinlay¹ 

Received: 6 April 2020 / Revised: 24 July 2020 / Accepted: 3 August 2020 / Published online: 12 August 2020
© The Author(s), under exclusive licence to International Society for Microbial Ecology 2020

Abstract

Interactive microbial communities are ubiquitous, influencing biogeochemical cycles and host health. One widespread interaction is nutrient exchange, or cross-feeding, wherein metabolites are transferred between microbes. Some cross-fed metabolites, such as vitamins, amino acids, and ammonium (NH_4^+), are communally valuable and impose a cost on the producer. The mechanisms that enforce cross-feeding of communally valuable metabolites are not fully understood. Previously we engineered a cross-feeding coculture between N_2 -fixing *Rhodospseudomonas palustris* and fermentative *Escherichia coli*. Engineered *R. palustris* excretes essential nitrogen as NH_4^+ to *E. coli*, while *E. coli* excretes essential carbon as fermentation products to *R. palustris*. Here, we sought to determine whether a reciprocal cross-feeding relationship would evolve spontaneously in cocultures with wild-type *R. palustris*, which is not known to excrete NH_4^+ . Indeed, we observed the emergence of NH_4^+ cross-feeding, but driven by adaptation of *E. coli* alone. A missense mutation in *E. coli* NtrC, a regulator of nitrogen scavenging, resulted in constitutive activation of an NH_4^+ transporter. This activity likely allowed *E. coli* to subsist on the small amount of leaked NH_4^+ and better reciprocate through elevated excretion of fermentation products from a larger *E. coli* population. Our results indicate that enhanced nutrient uptake by recipients, rather than increased excretion by producers, is an underappreciated yet possibly prevalent mechanism by which cross-feeding can emerge.

Introduction

Microorganisms typically exist as members of diverse and interactive communities wherein nutrient exchange, also known as cross-feeding, is thought to be ubiquitous [1–7]. The prevalence of cross-feeding might explain, in part, why

many microbes cannot synthesize essential vitamins and amino acids (i.e., auxotrophy), as they can often acquire these compounds from other community members [1, 7, 8]. Furthermore, microbes in nature experience varying degrees of starvation and often exist in a state of low metabolic activity [9, 10]. Thus, cross-feeding might also serve to sustain microbes through starvation. Despite the prevalence of cross-feeding, elucidating the molecular mechanisms underlying emergent cross-feeding interactions and tracking their evolutionary dynamics within natural microbial communities are difficult due to their sheer complexity. To overcome this intrinsic complexity, tractable synthetic consortia have proven useful for studying aspects of the mechanisms, ecology, evolution, and applications of microbial communities [4, 11–16].

To study the molecular mechanisms of nutrient cross-feeding, we previously developed a synthetic bacterial coculture in which *Escherichia coli* and *Rhodospseudomonas palustris* bidirectionally exchange essential metabolites under anaerobic conditions (Fig. 1a) [17–20]. In this coculture, *E. coli* ferments glucose, a carbon source that *R. palustris* cannot consume, and excretes ethanol and organic

Supplementary information The online version of this article (<https://doi.org/10.1038/s41396-020-00737-5>) contains supplementary material, which is available to authorized users.

✉ James B. McKinlay
jmckinla@indiana.edu

¹ Department of Biology, Indiana University, Bloomington, IN 47405, USA

² Department of Biochemistry and Molecular Biology, University of Arkansas for Medical Sciences, Little Rock, AR 72205, USA

³ School of Life Sciences, Biodesign Center for Mechanisms of Evolution, Arizona State University, Tempe, AZ 85281, USA

⁴ Department of Energy Joint Genome Institute, Walnut Creek, CA 94598, USA

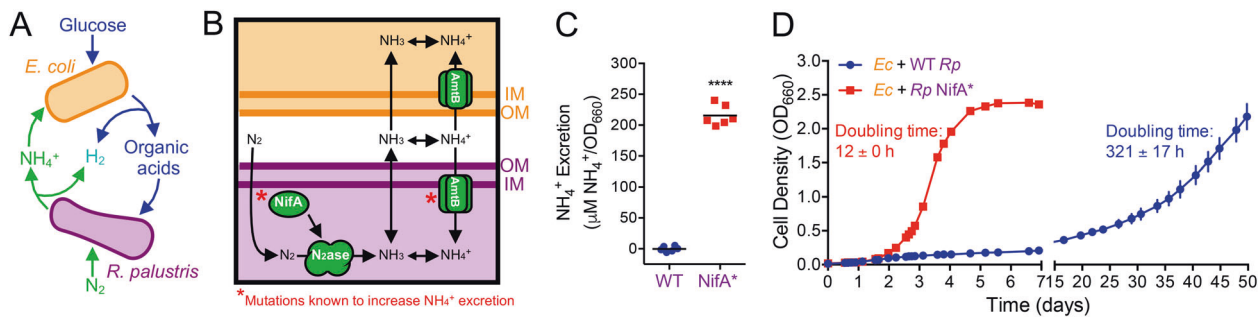


Fig. 1 Synergistic cross-feeding between *E. coli* and *R. palustris* is facilitated by NH_4^+ excretion. **a** Coculture growth requires reciprocal cross-feeding of organic acids and NH_4^+ excreted by *E. coli* and *R. palustris*, respectively. **b** Mechanism of NH_4^+ cross-feeding from *R. palustris* to *E. coli* and mutational targets known to increase NH_4^+ excretion by *R. palustris* (*). **c** NH_4^+ excretion levels by WT *R. palustris* (CGA009) and an isogenic *NifA** mutant (CGA676) in

acids, namely acetate, lactate, succinate, and formate, as waste products. The organic acids, with the exception of formate, serve as the sole carbon sources for *R. palustris* (Fig. 1a). In return, *R. palustris* fixes dinitrogen gas (N_2) via the enzyme nitrogenase and excretes ammonium (NH_4^+), which is the sole nitrogen source for *E. coli* (Fig. 1a). Because both species depend on essential nutrients provided by their partner, this coculture functions as a synthetic obligate mutualism.

NH_4^+ cross-feeding from *R. palustris* to *E. coli* is thought to depend on the equilibrium between NH_3 and NH_4^+ . The small proportion of NH_3 present in neutral pH environments is membrane permeable and can diffuse out of cells [21, 22]. Leaked NH_4^+ can be recaptured by AmtB transporters [21], which in the case of *R. palustris* helps privatize valuable NH_4^+ (Fig. 1b) [17, 18]. NH_4^+ leakage is also limited through the strict regulation of N_2 fixation, including by the transcriptional activator NifA, so that energetically expensive N_2 fixation is only performed when preferred nitrogen sources, such as NH_4^+ , are limiting [23]. Previously, we identified two types of mutations that increase NH_4^+ excretion by *R. palustris* during N_2 fixation and support coculture growth with *E. coli* [17]: (1) deletion of *amtB*, which prevents recapture of leaked NH_3 , or (2) a 48-bp deletion within *nifA* (denoted as *NifA**), which locks NifA into an active conformation [24] (Fig. 1b). In contrast, wild-type *R. palustris* does not readily support coculture growth with *E. coli* due to insufficient NH_4^+ excretion [17].

While synergistic cross-feeding of communally valuable NH_4^+ between *E. coli* and *R. palustris* can be rationally engineered, we questioned whether such an interaction could arise spontaneously. Herein we experimentally evolved cocultures pairing WT *E. coli* with either WT *R. palustris* or an engineered *NifA** mutant in serially transferred batch cultures for ~150 generations. In both cocultures, a reciprocal cross-feeding relationship was

established and growth rates improved over serial transfers, but growth and metabolic trends remained distinct. By pairing ancestral and evolved isolates of each species, we determined that adaptation by *E. coli* was solely responsible for establishing a synergistic relationship with WT *R. palustris*. Whole-genome sequencing and subsequent genetic verification identified a missense mutation in the *E. coli* transcriptional activator for nitrogen scavenging, NtrC, that was sufficient to enforce NH_4^+ cross-feeding with WT *R. palustris*. This mutation results in constitutive AmtB expression, presumably enhancing NH_4^+ uptake. Our results suggest that mutations that improve acquisition of communally valuable nutrients by recipients are favored to evolve and can promote the emergence of stable cross-feeding within synthetic consortia, and potentially within natural communities.

Material and methods

Bacterial strains and growth conditions

All strains and plasmids are listed in Supplementary Table S1. All *E. coli* strains used in this study are derived from the type strain MG1655 [25], unless noted otherwise. The WT and *NifA** *R. palustris* strains used in Fig. 1 were the type strain CGA009 [26] and CGA676, respectively. CGA676 carries a 48 bp deletion in *nifA* [24]. The *R. palustris* strains used in experimental coculture evolution and subsequent experiments were CGA4001 and CGA4003, which are derived from CGA009 and CGA676, respectively, with both carrying an additional $\Delta hupS$ mutation to prevent H_2 oxidation.

E. coli was grown in lysogeny broth (LB)-Miller (BD Difco) or on LB plates with 1.5% agar at 30 or 37 °C with gentamicin (Gm; 15 $\mu\text{g}/\text{ml}$), kanamycin (30 $\mu\text{g}/\text{ml}$),

or carbenicillin (Cb; 100 µg/ml) when appropriate. *R. palustris* was grown in defined minimal photosynthetic medium (PM) [26] or on PM agar with 10 mM succinate at 30 °C with Gm (100 µg/ml) when appropriate. N₂-fixing medium (NFM) was made by omitting (NH₄)₂SO₄ from PM. NFM and LB agar was used as selective media to quantify *R. palustris* and *E. coli* colony-forming units (CFUs), respectively. Experimental mono- and cocultures were grown in 10 ml of M9-derived coculture medium (MDC) in 27 ml anaerobic glass test tubes. Tubes were made anaerobic under 100% N₂, sterilized, and supplemented with 1 mM MgSO₄ and 0.1 mM CaCl₂ as described [17]. *E. coli* starter monocultures had 25 mM glucose and were growth-limited by supplementing with 1.5 mM NH₄Cl. *R. palustris* starter monocultures were growth-limited by supplementing with 3 mM acetate. Cocultures were inoculated by subculturing 1% v/v of starter monocultures of each species into MDC with 50 mM glucose. Mono- and cocultures were grown at 30 °C, under shaken conditions, lying horizontally and shaken at 150 rpm beneath a 60 W incandescent bulb (750 lumens), or under static conditions, standing vertically without shaking beside a 60 W incandescent bulb.

***E. coli* strain construction**

All primers are listed in Supplementary Table S2. To construct the *E. coli* NtrC^{S163R} mutant, the Gm^R-*sacB* genes from pJQ200SK [27] were PCR amplified using primers containing ~40 bp overhangs with homology up- and downstream of *ntrC* (*glnG*). A second round of PCR was subsequently performed to increase the length of overhanging regions of homology to ~80 bp to increase the recombination frequency. *E. coli* harboring pKD46, encoding arabinose-inducible λ-red recombineering genes [28], was grown in LB with 20 mM arabinose and Cb at 30 °C to an OD₆₀₀ of ~0.5 and then centrifuged, washed, and resuspended in sterile distilled water at ambient temperature. Resuspended cells were electroporated with the Gm^R-*sacB* PCR product containing overhangs flanking *ntrC* and plated on LB Gm agar. Gm-resistant colonies were screened by PCR for site-directed recombination of Gm^R-*sacB* into the *ntrC* locus, creating a Δ*ntrC*::Gm^R-*sacB* allele, which was then verified by sequencing. To replace the Δ*ntrC*::Gm^R-*sacB* locus, the NtrC^{S163R} allele was PCR amplified from gDNA from evolved *E. coli* (lineage A25) and electroporated into *E. coli* Δ*ntrC*::Gm^R-*sacB* harboring pKD46. After counterselection on LB agar with 10% (w/v) sucrose but without NaCl, site-directed recombination of the NtrC^{S163R} allele into the native locus was confirmed by PCR and sequencing. *E. coli* NtrC^{S163R} was grown overnight on LB agar at 42 °C to cure the strain of pKD46, which was confirmed by Cb sensitivity.

***R. palustris* strain construction**

To construct *R. palustris* CGA4001 and CGA4003, pJQ-Δ*hupS* was introduced into *R. palustris* CGA009 and CGA676, respectively, by conjugation with *E. coli* S17-1. Mutants were then obtained using sequential selection and screening as described [29]. The Δ*hupS* deletion was confirmed by PCR and sequencing.

Analytical procedures

Cell densities were approximated by optical density at 660 nm (OD₆₆₀) using a Genesys 20 visible spectrophotometer (Thermo-Fisher). Coculture doubling times were derived from specific growth rates determined by fitting exponential functions to OD₆₆₀ measurements between 0.1 and 1.0 for each biological replicate. NH₄⁺ was quantified using an indophenol colorimetric assay [17]. Glucose and soluble fermentation products were quantified by high-performance liquid chromatography (Shimadzu) as described [30]. H₂ was quantified by gas chromatography (Shimadzu) as described [31].

Coculture evolution experiments

Founder monocultures of *E. coli* MG1655, *R. palustris* CGA4001 (Δ*hupS*), and CGA4003 (Δ*hupS* NifA*) were inoculated from single colonies in MDC. Once grown, a single founder monoculture of each strain was used to inoculate 12 WT-based cocultures (six shaken: A–F; six static: G–L) and 12 NifA*-based cocultures (six shaken: M–R; six static: S–X) in MDC with 50 mM glucose. Cocultures were serially transferred by passaging 2% v/v of stationary phase coculture (OD₆₆₀ > 2 and a low metabolic rate based on H₂ measurements) into fresh MDC. The NifA*-based cocultures were transferred weekly, whereas WT-based cocultures were transferred every 21–50 days for the first five transfers and then approximately every 2 weeks based on the time required to reach OD₆₆₀ > 2. For comparative analyses, shaken cocultures (A–F and M–R) were revived from frozen stocks made following transfer-2 (generation 17) and transfer-25 (generation 146). Each frozen stock (~0.2 ml) was thawed in 1 ml sterile MDC, washed 2X with MDC to remove glycerol, and then resuspended in 0.2 ml MDC for use as inoculum.

RNA extraction and reverse transcription quantitative PCR (RT-qPCR)

RNA was isolated from exponentially growing *E. coli* monocultures or starved cell suspensions that had been chilled on ice, centrifuged at 4 °C, cell pellets frozen using dry ice in ethanol, and stored at –80 °C. Cell pellets were

thawed on ice, disrupted by bead beating, and then RNA was purified using an RNeasy MiniKit (Qiagen), Turbo DNase (Ambion) treatment on columns, and RNeasy MinElute Cleanup Kit (Qiagen). cDNA was synthesized from 0.5 to 1 µg of RNA per sample using Protoscript II RT and Random Primer Mix (New England Biolabs). qPCR reactions were performed on cDNA using iQ SYBR Green supermix (BioRad). *E. coli* gDNA was used to generate standard curves for *amtB* and *ntrC* transcript quantification, which were normalized to transcript levels of reference genes *gyrB* and *hcaT* [32]. Two technical replicate qPCR reactions were performed and averaged for each biological replicate to calculate relative expression.

Genome sequencing and mutation analysis

gDNA was extracted from stationary phase evolved cocultures following revival from frozen stocks using a Wizard Genomic DNA purification Kit (Promega). DNA fragment libraries were constructed for samples from shaking WT-based cocultures A–F and NifA*-based cocultures M–R at generation ~146 using NextFlex Bio Rapid DNA kit. Samples were sequenced on an Illumina NextSeq 500 150 bp paired-end run by the Indiana University Center for Genomics and Bioinformatics. Paired-end reads were trimmed using Trimmomatic 0.36 [33] with the following options: LEADING:3 TRAILING:3 SLIDINGWINDOW:10:26 HEADCROP:10 MINLEN:36. Mutations were called using *breseq* version 0.32.0 on Polymorphism Mode [34] and compared to a reference genome created by concatenating *E. coli* MG1655 (Accession NC_000913), *R. palustris* CGA009 (Accession BX571963), and its plasmid pRPA (Accession BX571964). Mutations are summarized in Supplementary File 1.

Additional gDNA sequencing for evolved WT-based cocultures A–F (shaking, generation 11), G–L (static, generations 11 and 123), and NifA*-based cocultures S–X (static, generation 123) was performed at the US Department of Energy Joint Genome Institute. Plate-based DNA library preparation for Illumina sequencing was performed on the PerkinElmer Sciclone NGS robotic liquid handling system using Kapa Biosystems library preparation kit. 200 ng of gDNA was sheared using a Covaris LE220 focused-ultrasonicator. Sheared DNA fragments were size selected by double-SPRI and selected fragments were end-repaired, A-tailed, and ligated with Illumina compatible sequencing adapters from IDT containing a unique molecular index barcode for each sample library. Libraries were quantified using KAPA Biosystem's next-generation sequencing library qPCR kit and run on a Roche LightCycler 480 real-time PCR instrument. The quantified libraries were then prepared for sequencing on the Illumina HiSeq sequencing platform utilizing a TruSeq Rapid paired-end cluster kit.

Sequencing was performed on the Illumina HiSeq2500 sequencer using HiSeq TruSeq SBS sequencing kits, following a 2 × 100 indexed run recipe. Reads were aligned to a reference genome created by concatenating *E. coli* MG1655 (Accession NC_000913), *R. palustris* CGA009 (Accession NC_005296), and its plasmid pRPA (Accession NC_005297) [35]. The resulting bam files were then split by organism and down sampled to 100-fold depth if in excess of that, then re-merged to create a normalized bam for calling single nucleotide polymorphisms and small indels by callVariants.sh from the BMap package (sourceforge.net/projects/bbmap/) to capture variants present within the population and annotation applied with snpEff [36]. Mutations are summarized in Supplementary File 2.

All FASTQ files are available at NCBI Sequence Read Archive (accession numbers listed in Supplementary Table S3).

Results

Emergence of nascent, synergistic cross-feeding between wild-type *R. palustris* and *E. coli*

Previously, we engineered *R. palustris* to excrete NH₄⁺ (NifA*) to stabilize mutualistic cross-feeding with *E. coli* (Fig. 1a, b). Here, we sought to determine whether such a relationship could evolve spontaneously. Spatial proximity has been shown to be an important factor in many microbial cross-feeding mutualisms [37–39], which can be disrupted by mixing. To account for the possible importance of proximity, we established cocultures with WT *R. palustris* (WT-based cocultures) under both shaken conditions, wherein cells are evenly distributed, and static conditions, wherein cells settle in close proximity at the bottom of the tube. In parallel, we also established shaken and static cocultures featuring the *R. palustris* NifA* strain (NifA*-based cocultures) as a comparative reference.

We confirmed our previous observations [17] that WT *R. palustris* exhibits undetectable NH₄⁺ excretion and does not readily support coculture growth with WT *E. coli*, in contrast to the NifA* mutant (Fig. 1c, d). Whereas shaken NifA*-based cocultures grew to an OD₆₆₀ > 2.0 in 4–6 days with a doubling time of ~12 h, shaken WT-based cocultures did not exhibit appreciable growth in the same time frame (Fig. 1d). We hypothesized that prolonged incubation might enrich for spontaneous mutants that permit coculture growth. Indeed, after 50 days, shaken WT-based cocultures reached densities similar to those observed for NifA*-based cocultures, albeit with a doubling time of ~13 days (Fig. 1d). Static WT- and NifA*-based cocultures also became turbid within similar time frames as their shaken counterparts.

Upon observing a nascent synergistic interaction between WT *R. palustris* and *E. coli*, we set up six replicate WT-based cocultures (A–F) and NifA*-based cocultures (M–R), all with WT *E. coli* (Fig. 2a), to experimentally

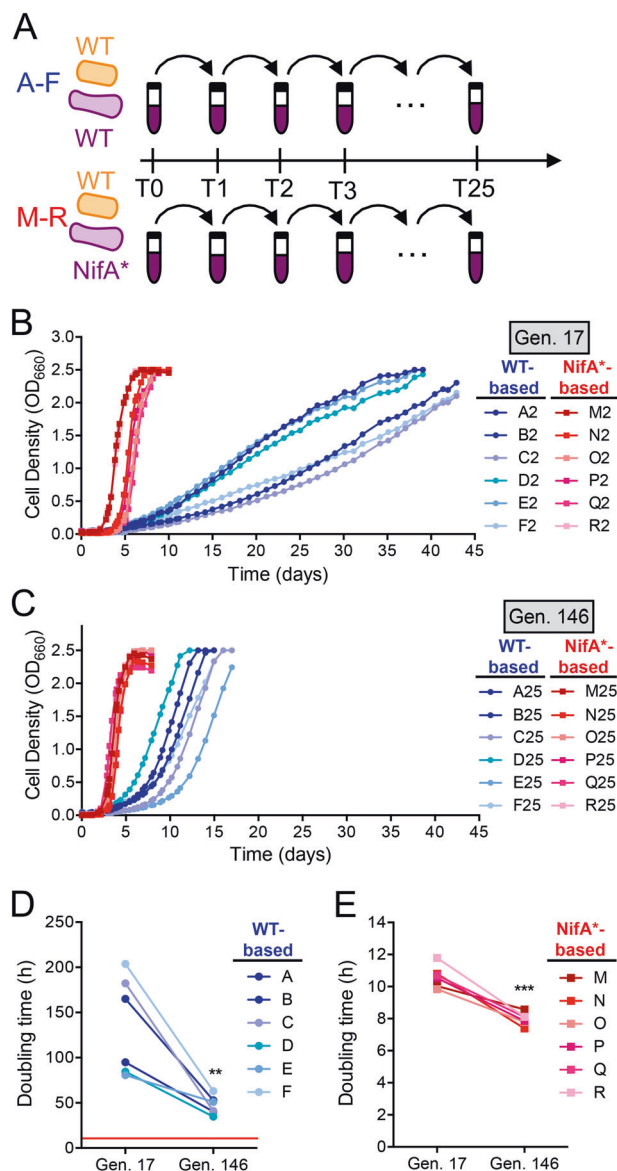


Fig. 2 Coculture doubling times decreased during experimental evolution of WT-based and NifA*-based cocultures. **a** Design for experimental evolution of parallel WT-based (A–F; CGA4001, derivative of WT/CGA009 with inactive hydrogenase) and NifA*-based (M–R; CGA4003, derivative of NifA*/CGA676 with inactive hydrogenase) cocultures via serial transfer (T#). Growth curves (both species) of WT-based and NifA*-based cocultures revived after two transfers (17 generations) (**b**) or 25 transfers (146 generations) (**c**) of experimental evolution. Points are values for the individual revived coculture lineages. Different shades indicate the different lineages. Coculture doubling times (both species) of individual WT-based cocultures (**d**) or NifA*-based cocultures (**e**) at generation (Gen.) 17 and 146, $n = 6$; two-tailed paired t -test, $**p < 0.01$, $t = 4$. $***p < 0.001$, $t = 8$. The red line in panel (**d**) indicates the mean doubling time of NifA*-based cocultures at gen. 17.

evolve through serial transfers under shaken conditions and compare their physiology, evolutionary trajectory, and species and genotypic composition. We also serially transferred static WT-based cocultures (G–L) and NifA*-based cocultures (S–X). The WT and NifA* *R. palustris* strains used in these coculture evolution experiments both have a deletion of the *hupS* gene, which inactivates hydrogenase and prevents H_2 oxidation, allowing us to quantify H_2 production. Herein, we focus the bulk of our analyses on shaken cocultures because (1) the close proximity provided under static conditions was not required for nascent cross-feeding, (2) shaken conditions facilitate analyses such as OD-based determination of growth rates, and (3) strong biofilms emerged in static cocultures, complicating the determination of population densities.

Shaken WT- and NifA*-based cocultures were serially transferred 25 times, corresponding to ~146 generations, with ~5.6 generations estimated per serial coculture (including the original cocultures designated, transfer-0) based on the 1:50 dilution used for each transfer. This number of generations corresponded to ~65 weeks for WT-based cocultures and ~26 weeks for NifA*-based cocultures. We then revived cocultures from frozen stocks made at transfer-2 (generation 17; G17) and transfer-25 (generation 146; G146) to compare growth and population trends. At G17, NifA*-based cocultures exceeded an OD_{660} of 2 in under 8 days, whereas WT-based cocultures took ~40 days (Fig. 2b). By G146, the time needed to reach $OD_{660} > 2$ had decreased for every lineage (Fig. 2c). The shortened growth phase was most pronounced for WT-based cocultures, which all reached $OD_{660} > 2$ in under 17 days by G146, less than half the time needed at G17 (Fig. 2b, c); WT-based coculture doubling times decreased from 135 ± 55 h to 47 ± 10 h (Fig. 2d). Though less drastic, NifA*-based coculture doubling times also decreased, in this case from ~11 to 8 h (Fig. 2e). Thus, WT-based cocultures adapted to grow faster, although never as fast as unevolved engineered NifA*-based cocultures.

Because growth trends differed between WT- and NifA*-based cocultures, we wondered how species populations were affected. We therefore enumerated viable cells as CFUs at the final time points for G17 and G146 cocultures shown in Fig. 2b, c. We describe several comparisons below using two-tailed t -tests ($n = 5$ –6; paired tests for G17 versus G146 comparisons and unpaired tests with Welch's correction for WT- versus NifA*-based coculture comparisons). At G17, *R. palustris* and *E. coli* populations in WT-based cocultures were, respectively, 0.15 ± 0.06 (SD; $p = 0.002$, $t = 7$) and 0.08 ± 0.04 -times (SD; $p = 0.0004$, $t = 10$) those in NifA*-based cocultures (Fig. 3a). It is worth noting that NifA*-based cocultures were plated after ~10 days, whereas WT-based cocultures were plated after 39–43 days due to their slower growth rate. Consequently, the lower

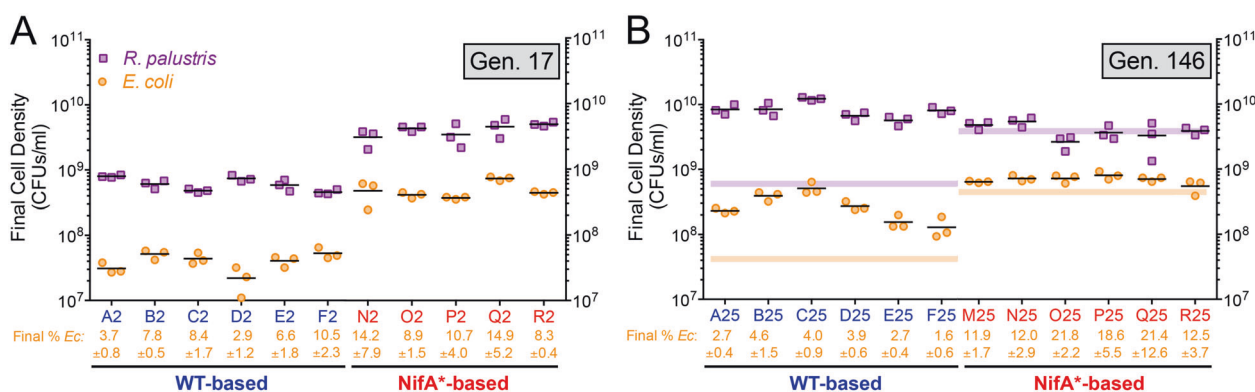


Fig. 3 Final populations in WT-based cocultures show large increases through serial transfers. **a, b** Final viable cell densities (colony-forming units [CFUs/ml]) of *R. palustris* and *E. coli* and the final *E. coli* percentage (\pm SD) at generation 17 (**a**) and generation 146 (**b**) for WT-based (CGA4001, derivative of WT/CGA009 with inactive hydrogenase) and NifA*-based (CGA4003, derivative of NifA*/

CGA676 with inactive hydrogenase) cocultures at the final time points shown in Fig. 2b, c. Points represent technical replicates of CFUs/ml for each lineage and lines are means, $n = 3$. The purple and orange lines in panel (**b**) indicate the median CFUs/ml for *R. palustris* and *E. coli*, respectively, at gen. 17 for reference. Data for lineage M at gen. 17 were unavailable due to agar contamination.

final populations in WT-based cocultures at G17 could be due in part to more background death and/or more resources spent on cellular maintenance. Increased death and maintenance in slow-growing cocultures is more likely to be an *E. coli* trait; *R. palustris* exhibits negligible death during starvation as it can cycle electrons to generate energy for maintenance when illuminated [40]. By G146, *R. palustris* abundances in WT-based cocultures had increased 14 ± 6 -fold (SD; $p = 0.001$, $t = 8$) and exceeded *R. palustris* abundances observed in NifA*-based cocultures at G146 by 2 ± 1 -fold (SD; $p = 0.004$, $t = 4$) (Fig. 3). *E. coli* abundances in WT-based cocultures also increased 8 ± 4 -fold (SD; $p = 0.010$, $t = 4$) by G146, but did not reach abundances observed in NifA*-based cocultures (Fig. 3). The increase in *E. coli* abundances in WT-based cocultures by G146 suggests that *E. coli* had better access to NH_4^+ , or other nitrogen compounds, than at G17 (Fig. 3b). Due to the disproportionate increase of each population in WT-based cocultures between G17 and G146, *E. coli* percentages remained low at 1–5%, relative to 11–22% in NifA*-based cocultures ($p = 0.001$, $t = 7$) (Fig. 3b). These differences in *E. coli* populations between WT- and NifA*-based cocultures are consistent with previous findings that higher NH_4^+ excretion by *R. palustris* supports faster growth and higher *E. coli* abundances [17–19].

In contrast to WT-based cocultures, NifA*-based cocultures did not display drastically higher cell densities for each species between G17 and G146 (Fig. 3). Average *R. palustris* densities were statistically similar between the two time points (1.0 ± 0.4 -fold change; SD; $p = 0.948$, $t = 0.1$). Average *E. coli* densities showed a small but significant increase between G17 and G146 (1.6 ± 0.4 -fold change; SD; $p = 0.009$, $t = 5$). However, the average *E. coli* percentage in NifA*-based cocultures showed less of a change between G17 (11.4%) and G146 (16.4%)

($p = 0.077$, $t = 2$) (Fig. 3). Although strong biofilms prevented us from accurately quantifying populations in static cocultures, we monitored the change in OD_{660} for each serial transfer between G20 and G100 (Fig. S1). Consistent with population trends in shaken cocultures, biomass formation fluctuated but generally increased for static WT-based cocultures but was relatively stable in static NifA*-based cocultures (Fig. S1).

Metabolic differences between WT- and NifA*-based cocultures help explain growth and population trends

Our past studies demonstrated that growth and population trends in coculture are strongly influenced by cross-feeding levels of both NH_4^+ and organic acids [17–19]. For instance, higher NH_4^+ cross-feeding to *E. coli* leads to higher *E. coli* growth rates [17–19]. In turn, higher *E. coli* growth rates boost organic acid excretion, supporting better *R. palustris* growth up until the organic acid excretion rate exceeds the rate at which *R. palustris* can consume them [17]. To see if such trends were also present in WT-based cocultures, we quantified glucose consumption and fermentation product yields at G17 and G146 at stationary phase. At G17, glucose consumption by *E. coli* in WT-based cocultures was about half of that in NifA*-based cocultures (Fig. 4a). The lower glucose consumption in WT-based cocultures can explain in part the lower *E. coli* CFUs observed in Fig. 3a. Previously, we showed that nongrowing *E. coli* can ferment glucose, and that this growth-independent fermentation can provide sufficient carbon to support *R. palustris* growth [19]. We hypothesize that growth-independent fermentation by *E. coli* was an important cross-feeding mechanism during the extremely slow growth of early WT-based cocultures (Fig. 1d).

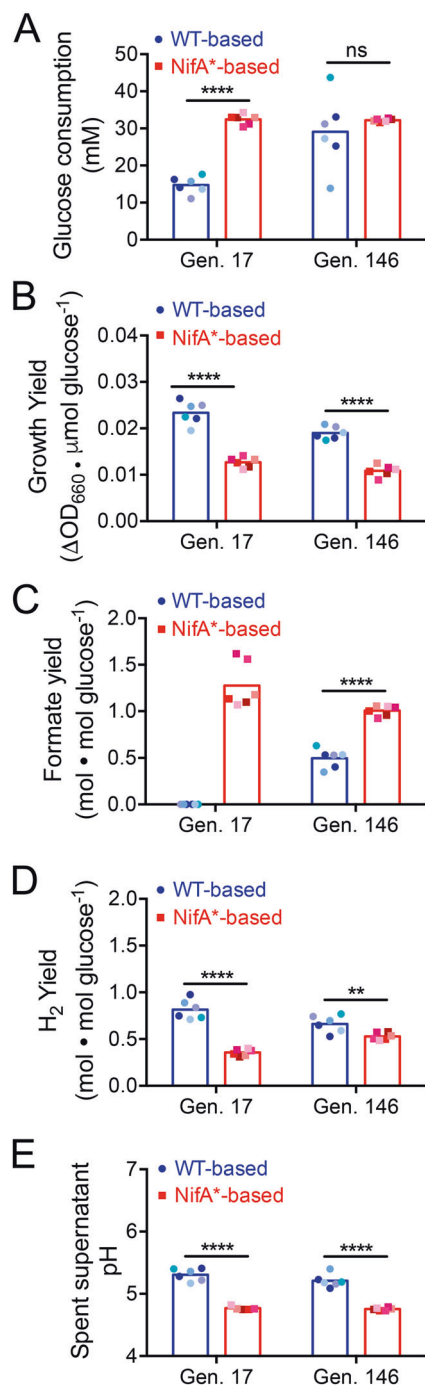


Fig. 4 WT-based and NifA*-based cocultures exhibit distinct metabolic phenotypes. Glucose consumption (a), growth yield (b), formate yield (c), H₂ yield (d), and final pH (e) for WT-based (CGA4001, derivative of WT/CGA009 with inactive hydrogenase) and NifA*-based (CGA4003, derivative of NifA*/CGA676 with inactive hydrogenase) revived coculture lineages at generation (Gen.) 17 and 146. Points are single measurements for individual lineages and bars are means, $n = 5-6$; multiple t -tests with Holm–Sidak post hoc test, $***p < 0.01$, $****p < 0.0001$. Different shades indicate different lineages. Metabolite measurements below detection limit were approximated to be 0. The pH of lineage P at Gen. 17 was not quantified because the culture tube broke prior to measurement.

However, by G146, *E. coli* glucose consumption in WT-based cocultures approached that in NifA*-based cocultures in most lineages, with one lineage consuming more glucose than NifA*-based cocultures (Fig. 4a). The general increase in *E. coli* glucose consumption in WT-based cocultures from G17 to G146 likely supported both the faster coculture doubling times (Fig. 2d) and higher *E. coli* abundances (Fig. 3b) and contributed to the accumulation of consumable organic acids such as acetate and succinate in some WT-based cocultures at G146, qualitatively similar to NifA*-based cocultures (Fig. S2). Overall, the increase in metabolic activities attributed to *E. coli* and the improved *E. coli* growth in WT-based cocultures between G17 and G146 suggest that nitrogen cross-feeding also increased.

We observed a potential trade-off between coculture growth rate and coculture growth yield ($\Delta OD_{660}/\text{glucose consumed}$). For example, WT-based G17 cocultures had the slowest growth rates but highest growth yields, whereas NifA*-based G146 cocultures had the fastest growth rates but lowest growth yields (Figs. 4b and S3). Trade-offs between growth rate and yield have been reported in multiple microbial species under various conditions [41–43]. In our case, the metabolic trends point to possible explanations for the apparent trade-off. For example, formate produced by *E. coli* is not consumed by *R. palustris* and thus typically accumulates in cocultures [17]. However, no formate was detected in WT-based G17 cocultures and formate yields were approximately half that of NifA*-based cocultures at G146 (Fig. 4c). Low formate yields could be explained in part by increased conversion of formate to H₂ and CO₂ by *E. coli* formate hydrogenlyase [44, 45]. Consistent with this possibility, WT-based cocultures had the highest H₂ yields (Fig. 4d). Low formate yields could also be explained by decreased formate production by *E. coli* in favor of other fermentation products. We previously observed low formate yields in slow-growing, nitrogen-limited NifA*-based cocultures [19, 20], suggesting that formate production by *E. coli* varies in response to growth rate. We have also not ruled out the possibility that *R. palustris* can consume some formate under certain conditions. In addition to formate, consumable organic acid yields were also lower at both G17 and G146 for WT-based cocultures relative to NifA*-based cocultures (Fig. S2). Organic acid accumulation in cocultures can acidify the medium to inhibitory levels [17]. At both G17 and G146, the lower yields of formate and other organic acids in WT-based cocultures were translated into higher pH values than in NifA*-based cocultures (Fig. 4e). This lower level of acidification combined with the likelihood of a higher proportion of glucose being fermented into organic acids other than formate could explain the higher *R. palustris* cell densities at G146 in WT-based cocultures compared to NifA*-based cocultures (Fig. 3b).

A single mutation in an *E. coli* nitrogen starvation response regulator is sufficient for synergistic growth with WT *R. palustris*

We hypothesized that the growth of WT-based cocultures was due to adaptive mutations in one or both species. To determine whether the evolution of either or both species was necessary to establish nascent reciprocal cross-feeding, we isolated single colonies of each species from ancestral WT populations and evolved G146 cocultures and paired them in all possible combinations (Fig. 5a). Only those pairings featuring evolved *E. coli* grew to an $OD_{660} > 0.5$ after ~24 days (Fig. 5b). Cocultures pairing evolved *E. coli* with ancestral or evolved WT *R. palustris* exhibited similar doubling times of ~67 h (Fig. S4). These results indicate that adaptation by *E. coli* alone is sufficient to establish a nascent mutualism with WT *R. palustris*. Accordingly, we did not observe increased NH_4^+ excretion in evolved WT *R. palustris* N_2 -fixing monocultures compared to the ancestral strain (Fig. S4).

To identify candidate mutations in *E. coli* that could drive improved coculture growth, we sequenced the genomes of populations in each evolved coculture lineage after 123–146 generations. We also sequenced WT-based cocultures following ~11 generations to determine if

potentially adaptive mutations arose early within WT-based cocultures. Several parallel mutations were identified in both species at frequencies between 5 and 100% (Table 1 and Supplementary Files 1 and 2). Consistent with evolved *E. coli* being necessary for mutualistic coculture growth with either ancestral or evolved WT *R. palustris* (Fig. 5b), we did not detect any *nifA* nor *amtB* mutations in evolved WT *R. palustris* populations, which would increase NH_4^+ excretion and enable rapid coculture growth. The multiple high frequency parallel mutations observed in evolved *R. palustris* populations (Table 1) are insufficient to improve coculture growth (Fig. 5b). Of the mutations in evolved *E. coli* populations, we were intrigued by a fixed missense mutation in *glnG* (henceforth called *ntrC*) that was fixed in all evolved *E. coli* populations from shaken WT-based cocultures and also occurred in the majority (4/6) of evolved static WT-based cocultures. This mutation in *ntrC* replaces serine 163 with an arginine within the AAA+ domain in the encoded response regulator NtrC (NtrC^{S163R}, Table 1 and Fig. 5c). NtrC and the histidine kinase NtrB form a two-component system that senses and coordinates the nitrogen starvation response in *E. coli* [46–48]. Our lab previously found that the *E. coli* NtrBC regulon is highly expressed in coculture with *R. palustris* NifA* [20]. Thus, *E. coli* NtrBC might be even more important in coculture with WT *R. palustris* wherein *E. coli* nitrogen starvation is expected to be intensified.

The NtrC^{S163R} mutation was enriched early in the evolution of WT-based cocultures, already at a high frequency in most lineages by G11 (Table 1 and Supplementary Table 3). Because of the striking parallelism of the NtrC^{S163R} mutation across coculture lineages, we wondered if it was present as standing genetic variation in the ancestral *E. coli* population. We therefore sequenced *ntrC* of ten *E. coli* isolates subjected to a single round (35 days) of coculture growth with WT *R. palustris* (Fig. 6a), which should enrich for the NtrC^{S163R} mutation. All ten isolates sequenced had the WT *ntrC* allele. Thus, although the NtrC^{S163R} allele was likely present in the founder population given its presence in every WT-based coculture lineage, it was under strong selection from an initial low frequency. In support of the importance of the NtrC^{S163R} allele, we also identified multiple, though different, high frequency mutations in *ntrB* and *ntrC* in *E. coli* populations from NifA*-based cocultures evolved under both well-mixed and static conditions (Table 1 and Supplementary Table 3). Together, these observations strongly suggest the adaptive importance of *E. coli* *ntrBC* mutations like NtrC^{S163R} for coculture growth, regardless of the NH_4^+ -excreting phenotype of the *R. palustris* partner.

To determine if the NtrC^{S163R} mutation alone was sufficient to support coculture growth with WT *R. palustris*, we moved the NtrC^{S163R} allele into the ancestral *E. coli* strain.

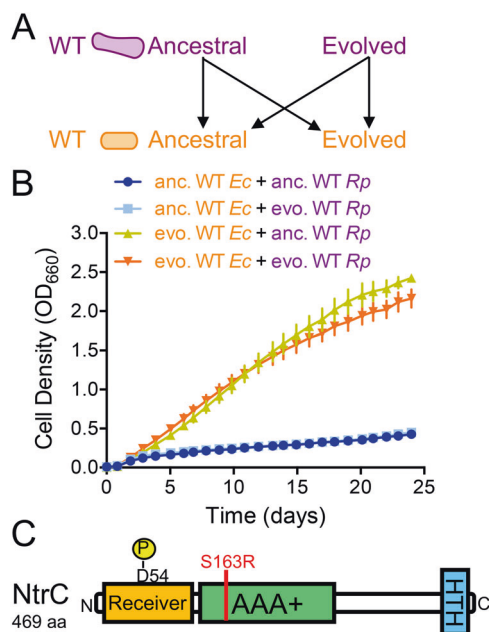


Fig. 5 Adaptation by *E. coli* is sufficient to enable growth of WT-based cocultures. Ancestral (anc) and evolved (evo) WT *R. palustris* (CGA4001, derivative of WT/CGA009 with inactive hydrogenase) and WT *E. coli* were paired in all possible combinations (a) and the growth of the cocultures (both species) was monitored (b). **b** Points are means \pm SEM, $n = 3$. **c** The location (red line) of the missense mutation in *E. coli* NtrC, which was fixed in all six parallel evolved *E. coli* populations from WT-based cocultures at G140–146.

Cocultures pairing *E. coli* NtrC^{S163R} with WT *R. palustris* grew with a doubling time of 124 ± 22 h, approximately twice as long as cocultures with evolved *E. coli* isolates, but much faster than cocultures with ancestral *E. coli* (Fig. 6a). Thus, the NtrC^{S163R} mutation is sufficient to drive coculture growth. Cocultures with *E. coli* NtrC^{S163R} reached similar final *E. coli* cell densities, but supported lower WT *R. palustris* abundances than cocultures with evolved *E. coli* isolates (Fig. 6b).

We speculate that some of the additional parallel mutations in evolved *E. coli* (Table 1) are also adaptive and account for the faster coculture growth rate relative to cocultures with the NtrC^{S163R} mutant (Fig. 6a). For example, the *E. coli* strain we used has a frameshift mutation in *rph* that decreases expression of *pyrE* immediately downstream [49]. Mutations in *rph* and in-between *rph* and *pyrE*, like those identified here (Table 1 and Supplementary Files 1 and 2), can improve pyrimidine biosynthesis and growth in minimal media [50]. HdfR is a transcriptional regulator that inhibits flagellar expression [51] and activates glutamate synthase expression [52]. HdfR loss-of-function mutations could reduce glutamate synthase expression and synchronize NH₄⁺ assimilation with the low NH₄⁺ cross-feeding levels in WT-based cocultures. However, the entire HdfR regulon has not been reported and thus could include other genes. In another possible link to nitrogen metabolism, mutations accumulated in the glutamine tRNA gene, *glnX* (Table 1). Two of the mutations disrupt the base-pair adjacent to the anticodon loop, while two others alter the anticodon, one still coding for glutamine but the other coding for histidine. The impact of these mutations is difficult to predict, especially since GlnX is just one of four *E. coli* tRNAs for glutamine. The *yhdWXYZ* operon encodes an NtrC-regulated amino acid ABC transporter, which is predicted to be nonfunctional due to a frameshift mutation in *yhdW* [46, 47]. The mutations identified in (Table 1) and directly upstream of the *yhdW* pseudogene (Supplementary Files 1 and 2) could restore amino acid transport for use as a nitrogen source or alternatively disrupt NtrC binding upstream of *yhdW* and thereby free up NtrC to regulate genes more critical to NH₄⁺ acquisition.

The *E. coli* NtrC^{S163R} allele constitutively activates ammonium transporter expression

Based on the effects of NtrC mutations observed by others [53, 54], we hypothesized that the NtrC^{S163R} allele facilitates coculture growth with WT *R. palustris* by conferring constitutive expression of NtrC-regulated genes important for NH₄⁺ acquisition. We previously determined that NtrC and AmtB were crucial gene products within the NtrC regulon for growth and coexistence with *R. palustris* NifA* [18, 20]. AmtB was one of the most important genes in the

NtrC regulon since overexpression of *amtB* rescued an *E. coli* Δ *ntrC* mutant in coculture [20]. To test if the NtrC^{S163R} allele increased *amtB* and *ntrC* expression, we measured transcript levels by RT-qPCR in *E. coli* monocultures grown with 15 mM NH₄Cl or subjected to complete nitrogen starvation (~10 h with 0 mM NH₄Cl). We chose to perform RT-qPCR on *E. coli* monocultures, because ancestral WT *E. coli* does not readily grow with WT *R. palustris* and because *E. coli* typically constitutes a low percentage (1–5%) of WT-based cocultures, meaning most mRNA would be from *R. palustris*.

When cultured with NH₄Cl, the *E. coli* NtrC^{S163R} mutant exhibited ~19 and 5-fold higher expression of *amtB* and *ntrC*, respectively, than WT *E. coli* (Figs. 6c and S5), indicating that the NtrC^{S163R} allele constitutively activates expression of its regulon. Following 10 h of nitrogen starvation, we saw similarly high *amtB* and *ntrC* expression by both the WT and the NtrC^{S163R} strains (Fig. 6c). Thus, both the WT and NtrC^{S163R} *E. coli* strains are able to commence strong transcriptional responses to extreme nitrogen starvation. We expect that the level of nitrogen limitation experienced by *E. coli* in coculture with WT *R. palustris* is less extreme than the complete nitrogen starvation conditions used in our qPCR experiments. Although we cannot detect NH₄⁺ excretion by WT *R. palustris*, the equilibrium with NH₃ dictates that some will be excreted, possibly within the nM to low μ M range where AmtB is critical [21]. We also know that AmtB is important in coculture for *E. coli* to compete for transiently available NH₄⁺ that *R. palustris* will otherwise reacquire [18]. We therefore hypothesize that the NtrC^{S163R} mutation primes *E. coli* for coculture growth with *R. palustris* by maintaining high AmtB expression and thereby increasing NH₄⁺ uptake rates at sub-saturating concentrations (Fig. S6). It is also possible that the NtrC^{S163R} mutation differentially regulates other genes beyond *amtB* that improve *E. coli* nitrogen acquisition or survival in coculture. Overall, our data suggest that a recipient species can stimulate cross-feeding through enhanced nutrient uptake.

Discussion

Here, we determined that in cocultures requiring nitrogen transfer from *R. palustris* to *E. coli*, an *E. coli* NtrC^{S163R} mutation alone is sufficient to enable coculture growth. The mutation results in constitutive activity of the NtrC regulon and thus increased expression of the AmtB NH₄⁺ transporter, which we hypothesize enhances NH₄⁺ uptake. This is the first mutation we have identified in the NH₄⁺ recipient *E. coli* that is sufficient to support synergistic growth with WT *R. palustris*. The faster growth and metabolism of *E. coli* resulting from the NtrC^{S163R} mutation should stimulate

faster organic acid excretion, which would, in turn, foster *R. palustris* growth and reciprocal NH_4^+ excretion. Thus, we envision that better NH_4^+ acquisition generates a positive feedback loop, enhancing the growth of both species. This positive feedback dynamic could transform a transient cross-feeding interaction into a burgeoning mutualistic relationship.

Our previous work on this consortium utilized *R. palustris* NifA* and ΔAmtB strains that we engineered to excrete NH_4^+ [17–19]. In the present study, we did not identify *nifA* or *amtB* mutations in evolved WT *R. palustris* populations. *R. palustris nifA* and *amtB* mutations likely incur a fitness cost, such as an increased energetic burden of constitutive nitrogenase expression due to the NifA* mutation or loss of NH_4^+ to WT competitors in the case of an inactivating *amtB* mutation. Thus, emergent *R. palustris nifA* and *amtB* mutants would not be expected to be competitive in the presence of a large WT *R. palustris* population. However, it does not appear that *R. palustris* NifA* regained regulation of nitrogenase, nor did it limit NH_4^+ excretion during the experimental evolution of NifA*-based cocultures. Instead, ancestral and evolved NifA*-based cocultures supported consistent abundances of *E. coli*, a trait that is dependent on the level of NH_4^+ excretion [17–19]. Our results therefore suggest that the NifA* mutation, a 48-bp deletion, is not prone to frequent or rapid suppression, at least during the time scale of this study, potentially because multiple mutations would be required. It is also possible that the cost of constitutive N_2 fixation is relatively low within this synthetic cross-feeding community. Based on our findings, we propose that experimental evolution of synthetic consortia is useful for both identifying novel genotypes enabling coexistence and assessing the stability of putatively costly engineered genotypes.

More broadly, our results indicate that within a cross-feeding partnership, multiple combinations of recipient and producer genotypes can lead to stable coexistence but only certain combinations will be favored based on the selective environment. We observed that both enhanced NH_4^+ excretion by the producer and enhanced NH_4^+ uptake by the recipient supported reciprocal cross-feeding, but only the latter emerged spontaneously. However, mutualistic excretion of costly nutrients could be selected for in other environments, such as those with strong spatial structuring. For example, costly methionine excretion and costly reciprocal galactose excretion sequentially evolved between *Salmonella enterica* and auxotrophic *E. coli* cocultured on agar plates [37, 39]. The limited mixing of populations on agar likely allowed for the reciprocal benefits to be preferentially directed to more cooperative genotypes [37, 39].

There is less likely to be selection for nutrient excretion under well-mixed conditions such as shaken liquid cultures because there is nearly equivalent access to limiting,

communally valuable nutrients, such as NH_4^+ [18], vitamins, and amino acids [1, 7, 8] between recipients and producers. Consequently, there is a probable fitness cost for producers associated with increased nutrient excretion in well-mixed environments because there is usually no way for an emergent more cooperative producer cell to direct nutrients to reciprocating recipients versus the less-cooperative ancestral producer. As a result, both costless self-serving mutations and mutually beneficial mutations, but not costly partner-serving mutations, are favored to evolve under well-mixed conditions [55]. Thus, mutations that improve a recipient's ability to acquire nutrients from producers, and thereby outcompete other recipient genotypes, can evolve rapidly [56]. Recipient mutations that enhance metabolite uptake also erode the partial privatization of communally valuable nutrients released by the producer [57]. Even so, these recipient mutations can eventually benefit producers if they promote a positive feedback loop of synergistic interactions [56].

We view the *E. coli* NtrC^{S163R} mutation as an example of a self-serving mutation, given its rapid emergence in shaken cocultures, but one that is mutually beneficial in the context of an obligate cross-feeding relationship. We hypothesize that the benefit of the NtrC^{S163R} mutation for *E. coli* extends more generally to surviving nitrogen limitation. In support of this, an NtrC^{V18L} mutation that similarly increased *amtB* expression was adaptive for *E. coli* evolved in nitrogen-limiting monocultures [58]. *E. coli* is nitrogen limited in all coculture conditions used in this study, likely explaining why other *E. coli* NtrBC mutations were frequently observed in evolved NifA*-based cocultures, and in most static cocultures, where the dense populations at the bottom of the test tube may intensify competition for NH_4^+ . We did not identify any clear examples of costly metabolite excretion in static WT-based cocultures, perhaps because the level of spatial structure was insufficient to favor such mutations compared to lawns on agar plates [37, 39].

Mutations that improve nutrient acquisition can be mutually beneficial for cross-feeding partners under conditions where neither species can grow well without reciprocal nutrient exchange. However, mutations that enhance nutrient uptake could also be adaptive for the recipient when there is no reciprocal benefit to the producer. For example, acetate cross-feeding repeatedly evolved in *E. coli* populations under glucose-limiting conditions through mutations that enhanced acetate uptake by a nascent recipient subpopulation [59, 60]. Unlike in our study, the acetate-consuming recipients did not provide a clear reciprocal benefit to the acetate-excreting producers, beyond potentially relaxing competition for glucose due to resource partitioning [59, 60]. Thus, mutations that enhance nutrient uptake could foster the emergence of mutualistic, commensal, or competitive interactions, depending on

community composition and conditions [56, 59, 60]. In natural microbial communities, where auxotrophy is prevalent [1, 7] and most cells exhibit low metabolic activity [9, 10], mutations that improve acquisition of limiting nutrients could allow certain populations to flourish. Understanding the consequences of mutations that expedite metabolite acquisition could thus inform on the origins of various ecological relationships. This knowledge could ultimately be harnessed for applications ranging from facilitating coexistence within synthetic consortia to probiotic-mediated competitive exclusion of pathogens.

Acknowledgements This work was supported in part by the US Army Research Office grants W911NF-14-1-0411 and W911NF-17-1-0159, a National Science Foundation CAREER award MCB-1749489, the US Department of Energy, Office of Science, Office of Biological and Environmental Research, under award DE-SC0008131, and the Joint Genome Institute Community Science Program, CSP 502893. The work conducted by the US Department of Energy Joint Genome Institute, a DOE Office of Science User Facility, is supported by the Office of Science of the US Department of Energy under Contract No. DE-AC02-05CH11231. We thank A.L. Posto, J.R. Gliessman, and M.C. Onyeziri for coculture passaging and initial characterizations, J.T. Lennon and B.K. Lehmkuhl for equipment and assistance with qRT-PCR, and J. Ford and A.M. Buechlein at the IU Center for Genomics and Bioinformatics.

Compliance with ethical standards

Conflict of interest The authors declare that they have no conflict of interest.

Publisher's note Springer Nature remains neutral with regard to jurisdictional claims in published maps and institutional affiliations.

References

- Seth EC, Taga ME. Nutrient cross-feeding in the microbial world. *Front Microbiol.* 2014;5:350.
- Estrela S, Trisos CH, Brown SP. From metabolism to ecology: cross-feeding interactions shape the balance between poly-microbial conflict and mutualism. *Am Nat.* 2012;180:566–76.
- Morris BEL, Henneberger R, Huber H, Moissl-Eichinger C. Microbial syntrophy: interaction for the common good. *FEMS Microbiol Rev.* 2013;37:384–406.
- Ponomarova O, Patil KR. Metabolic interactions in microbial communities: untangling the Gordian knot. *Curr Opin Microbiol.* 2015;27:37–44.
- Zelezniak A, Andrejev S, Ponomarova O, Mende DR, Bork P, Patil KR. Metabolic dependencies drive species co-occurrence in diverse microbial communities. *Proc Natl Acad Sci USA.* 2015;112:6449–54.
- Emree M, Liu JK, Al-Bassam MM, Zengler K. Networks of energetic and metabolic interactions define dynamics in microbial communities. *Proc Natl Acad Sci USA.* 2015;112:15450–5.
- Zengler K, Zaramela LS. The social network of microorganisms—how auxotrophies shape complex communities. *Nat Rev Microbiol.* 2018;16:383–90.
- Mee MT, Collins JJ, Church GM, Wang HH. Syntrophic exchange in synthetic microbial communities. *Proc Natl Acad Sci USA.* 2014;111:E2149–56.
- Bergkessel M, Basta DW, Newman DK. The physiology of growth arrest: uniting molecular and environmental microbiology. *Nat Rev Microbiol.* 2016;14:549–62.
- Lennon JT, Jones SE. Microbial seed banks: the ecological and evolutionary implications of dormancy. *Nat Rev Microbiol.* 2011;9:119–30.
- Momeni B, Chen C-C, Hillesland KL, Waite A, Shou W. Using artificial systems to explore the ecology and evolution of symbioses. *Cell Mol Life Sci.* 2011;68:1353–68.
- Mee MT, Wang HH. Engineering ecosystems and synthetic ecologies. *Mol Biosyst.* 2012;8:2470–83.
- Lindemann SR, Bernstein HC, Song H-S, Fredrickson JK, Fields MW, Shou W, et al. Engineering microbial consortia for controllable outputs. *ISME J.* 2016;10:2077–84.
- Widder S, Allen RJ, Pfeiffer T, Curtis TP, Wiuf C, Sloan WT, et al. Challenges in microbial ecology: building predictive understanding of community function and dynamics. *ISME J.* 2016;10:2557–68.
- Hillesland KL, Stahl DA. Rapid evolution of stability and productivity at the origin of a microbial mutualism. *Proc Natl Acad Sci USA.* 2010;107:2124–9.
- Harcombe WR, Riehl WJ, Dukovski I, Granger BR, Betts A, Lang AH, et al. Metabolic resource allocation in individual microbes determines ecosystem interactions and spatial dynamics. *Cell Rep.* 2014;7:1104–15.
- LaSarre B, McCully AL, Lennon JT, McKinlay JB. Microbial mutualism dynamics governed by dose-dependent toxicity of cross-fed nutrients. *ISME J.* 2016;11:337–48.
- McCully AL, LaSarre B, McKinlay JB. Recipient-biased competition for an intracellularly generated cross-fed nutrient is required for coexistence of microbial mutualists. *mBio.* 2017;8:e01620–17.
- McCully AL, LaSarre B, McKinlay JB. Growth-independent cross-feeding modifies boundaries for coexistence in a bacterial mutualism. *Environ Microbiol.* 2017;19:3538–50.
- McCully AL, Behringer MG, Gliessman JR, Pilipenko EV, Mazny JL, Lynch M, et al. An *Escherichia coli* nitrogen starvation response is important for mutualistic coexistence with *Rhodospseudomonas palustris*. *Appl Environ Microbiol.* 2018;84:e00404–18.
- Kim M, Zhang Z, Okano H, Yan D, Groisman A, Hwa T. Need-based activation of ammonium uptake in *Escherichia coli*. *Mol Syst Biol.* 2012;8:616.
- Walter A, Gutknecht J. Permeability of small nonelectrolytes through lipid bilayer membranes. *J Membr Biol.* 1986;90:207–17.
- Dixon R, Kahn D. Genetic regulation of biological nitrogen fixation. *Nat Rev Microbiol.* 2004;2:621–31.
- McKinlay JB, Harwood CS. Carbon dioxide fixation as a central redox cofactor recycling mechanism in bacteria. *Proc Natl Acad Sci USA.* 2010;107:11669–75.
- Blattner FR, Plunkett G, Bloch CA, Perna NT, Burland V, Riley M, et al. The complete genome sequence of *Escherichia coli* K-12. *Science.* 1997;277:1453–62.
- Kim M-K, Harwood CS. Regulation of benzoate-CoA ligase in *Rhodospseudomonas palustris*. *FEMS Microbiol Lett.* 1991;83:199–203.
- Quandt J, Hynes MF. Versatile suicide vectors which allow direct selection for gene replacement in Gram-negative bacteria. *Gene.* 1993;127:15–21.
- Datsenko KA, Wanner BL. One-step inactivation of chromosomal genes in *Escherichia coli* K-12 using PCR products. *Proc Natl Acad Sci USA.* 2000;97:6640–5.
- Rey FE, Oda Y, Harwood CS. Regulation of uptake hydrogenase and effects of hydrogen utilization on gene expression in *Rhodospseudomonas palustris*. *J Bacteriol.* 2006;188:6143–52.

30. McKinlay JB, Zeikus JG, Vieille C. Insights into *Actinobacillus succinogenes* fermentative metabolism in a chemically defined growth medium. *Appl Environ Microbiol.* 2005;71:6651–6.
31. Huang JJ, Heiniger EK, McKinlay JB, Harwood CS. Production of hydrogen gas from light and the inorganic electron donor thiosulfate by *Rhodospseudomonas palustris*. *Appl Environ Microbiol.* 2010;76:7717–22.
32. Zhou K, Zhou L, Lim QE, Zou R, Stephanopoulos G, Too H-P. Novel reference genes for quantifying transcriptional responses of *Escherichia coli* to protein overexpression by quantitative PCR. *BMC Mol Biol.* 2011;12:18.
33. Bolger AM, Lohse M, Usadel B. Trimmomatic: a flexible trimmer for Illumina sequence data. *Bioinformatics.* 2014;30:2114–20.
34. Deatherage DE, Barrick JE. Identification of mutations in laboratory-evolved microbes from next-generation sequencing data using breseq. In: Sun L, Shou W, editors. *Engineering and analyzing multicellular systems: methods and protocols.* New York, NY: Springer New York; 2014. p. 165–88.
35. Li H, Durbin R. Fast and accurate short read alignment with Burrows–Wheeler transform. *Bioinformatics.* 2009;25:1754–60.
36. Cingolani P, Platts A, Wang LL, Coon M, Nguyen T, Wang L, et al. A program for annotating and predicting the effects of single nucleotide polymorphisms, SnpEff. *Fly.* 2012;6:80–92.
37. Harcombe WR, Chacón JM, Adamowicz EM, Chubiz LM, Marx CJ. Evolution of bidirectional costly mutualism from byproduct consumption. *Proc Natl Acad Sci USA.* 2018;115:12000–4.
38. Pande S, Kaftan F, Lang S, Svatoš A, Germerodt S, Kost C. Privatization of cooperative benefits stabilizes mutualistic cross-feeding interactions in spatially structured environments. *ISME J.* 2015;10:1413–23.
39. Harcombe W. Novel cooperation experimentally evolved between species. *Evolution.* 2010;64:2166–72.
40. Pechter KB, Yin L, Oda Y, Gallagher L, Yang J, Manoil C, et al. Molecular basis of bacterial longevity. *mBio.* 2017;8:e01726–17.
41. Lipson DA. The complex relationship between microbial growth rate and yield and its implications for ecosystem processes. *Front Microbiol.* 2015;6:615.
42. Wortel MT, Noor E, Ferris M, Bruggeman FJ, Liebermeister W. Metabolic enzyme cost explains variable trade-offs between microbial growth rate and yield. *PLoS Comp Biol.* 2018;14:e1006010.
43. Cheng C, O'Brien EJ, McCloskey D, Utrilla J, Olson C, LaCroix RA, et al. Laboratory evolution reveals a two-dimensional rate-yield tradeoff in microbial metabolism. *PLoS Comp Biol.* 2019;15:e1007066.
44. McDowall JS, Murphy BJ, Haumann M, Palmer T, Armstrong FA, Sargent F. Bacterial formate hydrogenlyase complex. *Proc Natl Acad Sci USA.* 2014;111:E3948–56.
45. Sangani AA, McCully AL, LaSarre B, McKinlay JB. Fermentative *Escherichia coli* makes a substantial contribution to H₂ production in coculture with phototrophic *Rhodospseudomonas palustris*. *FEMS Microbiol Lett.* 2019;366:fnz162.
46. Zimmer DP, Soupene E, Lee HL, Wendisch VF, Khodursky AB, Peter BJ, et al. Nitrogen regulatory protein C-controlled genes of *Escherichia coli*: scavenging as a defense against nitrogen limitation. *Proc Natl Acad Sci USA.* 2000;97:14674–9.
47. Brown DR, Barton G, Pan Z, Buck M, Wigneshweraraj S. Nitrogen stress response and stringent response are coupled in *Escherichia coli*. *Nat Commun.* 2014;5:4115.
48. Switzer A, Brown DR, Wigneshweraraj S. New insights into the adaptive transcriptional response to nitrogen starvation in *Escherichia coli*. *Biochem Soc Trans.* 2018;46:1721–8.
49. Jensen KF. The *Escherichia coli* K-12 “wild types” W3110 and MG1655 have an *rph* frameshift mutation that leads to pyrimidine starvation due to low *pyrE* expression levels. *J Bacteriol.* 1993;175:3401–7.
50. LaCroix RA, Sandberg TE, O'Brien EJ, Utrilla J, Ebrahim A, Guzman GI, et al. Use of adaptive laboratory evolution to discover key mutations enabling rapid growth of *Escherichia coli* K-12 MG1655 on glucose minimal medium. *Appl Environ Microbiol.* 2015;81:17–30.
51. Ko M, Park C. H-NS-Dependent regulation of flagellar synthesis is mediated by a LysR family protein. *J Bacteriol.* 2000;182:4670–2.
52. Krin E, Danchin A, Soutourina O. Decrypting the H-NS-dependent regulatory cascade of acid stress resistance in *Escherichia coli*. *BMC Microbiol.* 2010;10:273.
53. Weglenski P, Ninfa AJ, Ueno-Nishio S, Magasanik B. Mutations in the *glnG* gene of *Escherichia coli* that result in increased activity of nitrogen regulator I. *J Bacteriol.* 1989;171:4479–85.
54. Dixon R, Eydmann T, Henderson N, Austin S. Substitutions at a single amino acid residue in the nitrogen-regulated activator protein NTRC differentially influence its activity in response to phosphorylation. *Mol Microbiol.* 1991;5:1657–67.
55. Hart SFM, Pineda JMB, Chen C-C, Green R, Shou W. Disentangling strictly self-serving mutations from win-win mutations in a mutualistic microbial community. *eLife.* 2019;8:e44812.
56. Waite AJ, Shou W. Adaptation to a new environment allows cooperators to purge cheaters stochastically. *Proc Natl Acad Sci USA.* 2012;109:19079–86.
57. Estrela S, Morris JJ, Kerr B. Private benefits and metabolic conflicts shape the emergence of microbial interdependencies. *Environ Microbiol.* 2016;18:1415–27.
58. Warsi OM, Andersson DI, Dykhuizen DE. Different adaptive strategies in *E. coli* populations evolving under macronutrient limitation and metal ion limitation. *BMC Evol Biol.* 2018;18:72.
59. Rosenzweig RF, Sharp RR, Treves DS, Adams J. Microbial evolution in a simple unstructured environment: genetic differentiation in *Escherichia coli*. *Genetics.* 1994;137:903–17.
60. Treves DS, Manning S, Adams J. Repeated evolution of an acetate-crossfeeding polymorphism in long-term populations of *Escherichia coli*. *Mol Biol Evol.* 1998;15:789–97.